# DEVELOPMENT OF HIGH TEMPERATURE TARGETS AND ION SOURCES FOR ON-LINE RADIOACTIVE ISOTOPE PRODUCTION

**V.N.Panteleev, A.E.Barzakh, D.V.Fedorov, V.S.Ivanov, F.V.Moroz, S.Yu.Orlov, A.G.Polyakov, M.D.Seliverstov, Yu.M.Volkov**

## 1. Introduction

At the IRIS facility a high temperature target for effective production of a large set of short lived nuclides was worked out and used for on-line experiments [1]. The use of a tungsten foil as a target container material allows to maintain the working temperature for refractory foil and refractory metal carbide targets up to 2800–3000°C and up to 2500°C for uranium carbide targets. Tests of Ta, Ta-W, TaC, NbC and UC target materials in a tungsten container in the temperature interval of 2400–3000°C demonstrated a high reliability of used targets during long (of about 100 hours) on-line runs. A large set of the neutron deficient and the neutron rich nuclides were produced making use the developed target. From a high temperature refractory target with a tantalum foil as a target material the isotopes of practically all rare-earth elements were produced. That target was used for laser spectroscopic investigations of chains of Yb and Tm neutron deficient isotopes.

A number of on-line and off-line tests of high temperature uranium carbide targets of different density were carried out. High yields of Rb and Cs neutron rich isotopes were obtained from uranium carbide powder target and from uranium carbide target of a high density. The experimental results have been obtained which clearly demonstrate the influence of the neutron generation effect on the yields of produced isotopes. In these experiments a tantalum block, placed close by the uranium carbide target of a low density, served as a generator for a secondary neutron production. Considerable rise of Cs and Rb neutron rich isotopes produced in two step reaction were measured in comparison with production in the target directly irradiated by protons.

A production gain of neutron rich Cs and In isotopes was measured as well from a high density uranium carbide target (11 g/cm$^3$) as compared to uranium carbide powder target of lower density (3.1 g/cm$^3$). It has been confirmed that a high density uranium carbide target can serve itself as a rather effective generator of secondary neutrons inside the target material volume.

Different types of ion sources for efficient and selective isotope production have been developed and on-line tested.

A surface ionization ion source demonstrates the ionization efficiency values from 1% to 100% for elements with ionization potentials from 6.2 eV to 4 eV. The ion sources of this type were used for production and investigation of isotopes of alkali and rare-earth elements.

Laser ion source, firstly developed [1] and on-line tested [2] at the IRIS facility, makes possible the efficient isobar separation and provides the ionization efficiency in the range of 1–10% for the isotopes of a number elements of the periodical table. For the first time as well at the IRIS facility the laser spectroscopy inside the laser ion source has been applied and demonstrated a very high sensitivity of measurements [3].

A new developed and on-line tested high temperature electron bombardment ion source can be used for production of all isotopes of the nuclide chart with the efficiency of 1–20%, when the chemical selectivity is not necessary. During the first on-line run with that type of ion source use the neutron rich isotopes of Mn, Ag, Cd, In and Sn and neutron deficient ones of Tl, Pb, Bi, Po and At were produced and identified by $\gamma$-spectra measurements.

## 2. High temperature refractory metal and refractory metal carbide targets

### 2.1. Off-line tests of a high temperature tantalum target unit

In Fig. 1 a high temperature target unit with a tantalum foil as a target material is presented.

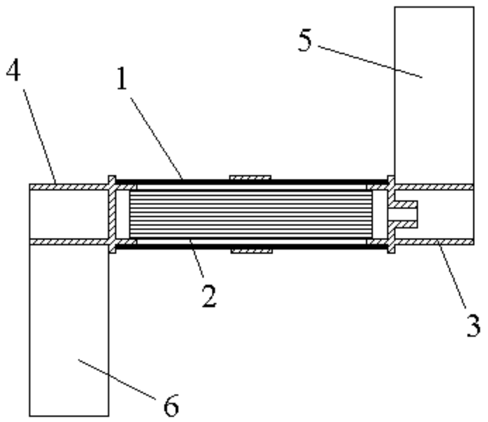


**Fig. 1.** Conceptual scheme of a high temperature target unit with a tantalum foil as a target material. 1– target container made of the rolled tungsten foils of 45 mm long, 10 mm in diameter, 0.2–0.4 mm wall thickness; 2 – target material: 20 $\mu$m and 4 $\mu$m Ta or W foils are used; 3,4 – tantalum plugs; 5,6 – flexible tantalum connectors

Some off-line tests have been carried out at the IRIS mass-separator. In Fig. 2 (left plot) temperature distribution along the target container is presented. The temperature determination error does not exceed 20°C. Measurements have shown that the temperature difference between the target ends and the target center does not exceed 250°C.

In Fig. 2 (right plot) emissivity value of the tungsten target container is shown. Emissivity characterizes the power dissipation efficiency of a target unit. Power, dissipated by the target container at temperature $T$ to the surrounding enclosure at temperature $T_0$, is given by:

$$P = \varepsilon \cdot \kappa \cdot A(T^4 - T_o^{\,4})F,$$

where $\varepsilon$ – total emissivity, $\kappa$ – Boltzmann's constant, $A$ – the emitting area and $F$ – geometrical factor. For an enclosure that is large compared to the IRIS target container, $F$ is unity [4]. $P$ was determined by the electrical heating power contributed to the target. Calculated tungsten container emissivity was about 0.6 in the wide range of temperatures. To compare, the tantalum container emissivity is of 0.3 (see P.V.Drumm *et al,* Nucl. Instr. Meth. **B126**, 121 (1997)).

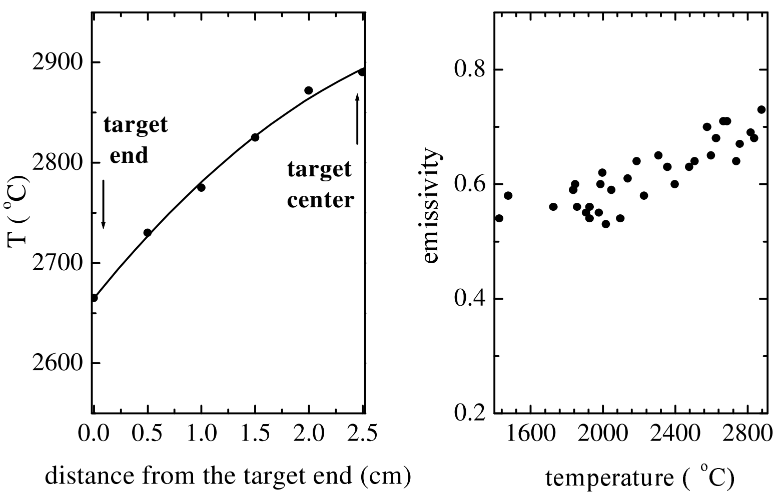


**Fig. 2.** Temperature distribution along the target (left plot) and emissivity of a tungsten container (right plot)

The off-line and on-line tests have shown that the target container surface does not change its emissivity during the time of experiment (of about 70–100 hours). The obtained emissivity value and value of power dissipated by high temperature targets of different dimensions bring us to a conclusion that there is a real possibility to construct a high temperature target unit with an effective utilisation of a proton beam of the energy 0.5–2 GeV, which incorporates into the target the power of about 30 kW, avoiding the target destruction due to overheating.

### 2.2. On-line tests of a high temperature refractory target. Yields and release of lithium isotopes

Taking into account all investigated properties of the IRIS high temperature target, the next scheme has been chosen for on-line experiment. Target has been installed perpendicularly to the proton beam (see Fig.3). At this geometry temperature distribution along the working area of the target can be considered as a constant. The mass of target material in the working area was 5 g/cm$^2$ of Ta and W 20 $\mu$m thick foils.

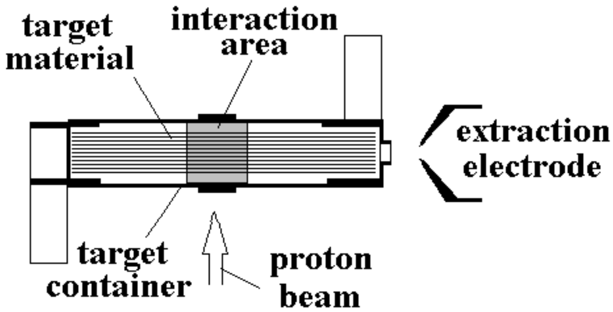


**Fig. 3.** On-line experiment arrangement

We did not use an ion source for alkali radioactive ion production, because the ionization efficiency inside the high temperature target itself at the working temperature about 2800°C was high enough [4]. An electron multiplier has been applied for the lithium release curve and yield measurements.

In Fig. 4 the release curve of radiogenic $^6$Li is shown obtained by switching off the proton beam and collecting radioactive samples during equal (3 s) time intervals.

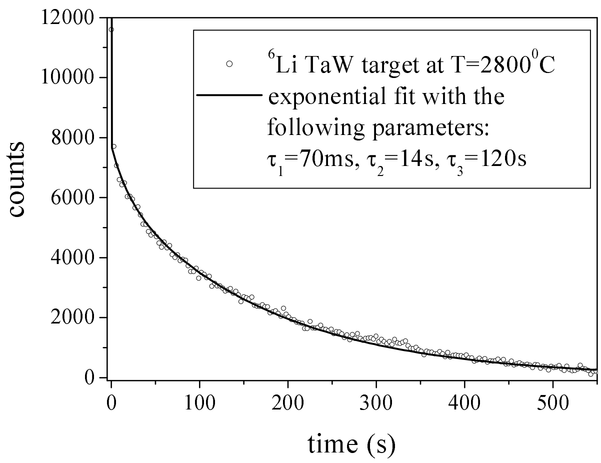


**Fig. 4.** Release curve of radiogenic $^6$Li from the IRIS target unit. Fitting curve: $F(t)=A_1{\cdot}e^{-\lambda_1 \cdot t}+A_2{\cdot}e^{-\lambda_2 \cdot t}+(1-A_1-A_2){\cdot}e^{-\lambda_3 \cdot t}$ has been used, where $\lambda_i=ln2/\tau_i$ are release constants

Short delay time (of about 70 ms) in the fitting curve is taking from special measurements of the short release component between the proton bunches [4]. Yields of radioactive Li isotopes are presented in Table 1.

*Table 1*

Yields of lithium isotopes from IRIS high temperature target

| ISOTOPE | Half-life, ms | IRIS $5 g/cm^2$, 0.1 $\mu A$ (experimental data) | ISOLDE 149 $g/cm^2$, 1 $\mu A$ (experimental data) | IRIS* scaled to 120 $g/cm^2$, 1 $\mu A$ |
|---|---|---|---|---|
| $^{8}Li$ | 840 | $6\times10^{6}\ s^{-1}$ | $1.5\times10^{7}\ s^{-1}$ | $1.4\times10^{9}\ s^{-1}$ |
| $^{9}Li$ | 179 | $3\times10^{5}\ s^{-1}$ | $5.4\times10^{5}\ s^{-1}$ | $7.2\times10^{7}\ s^{-1}$ |
| $^{11}Li$ | 8.3 | $5\times10^{2}\ s^{-1}$ | $2.5\times10^{3}\ s^{-1}$ | $1.2\times10^{5}\ s^{-1}$ |

*to compare IRIS and ISOLDE targets, the experimental yields from small IRIS target were scaled to the usual ISOLDE target mass and proton beam intensity

The main task when building a full scale target is to avoid appearance of cold spots inside the target container. Presently, the 18 $g/cm^2$ target has been successfully used by laser group of IRIS facility for isotope shift and hyperfine structure investigations [5].

In Fig. 5 release curves of radiogenic $^{6}Li$ from Ta and Ta-W foil targets are shown. Ta-W foil target was built as a sandwich to protect Ta foils against sticking. For the same purpose 3 $\mu$m thick foils were placed into a graphite container. In both cases targets conserved their parameters (the value of Li yields and delay time) during all time of the experiment (of about 80–100 hours). As it is seen from Fig. 5, the relation between delay times of different target materials: 199 s (80%) at 20 $\mu$m foils and 5 s (90%) at 3 $\mu$m foils is in a good agreement with the value expected from the Fick's diffusion equation and approximately equal to 40.

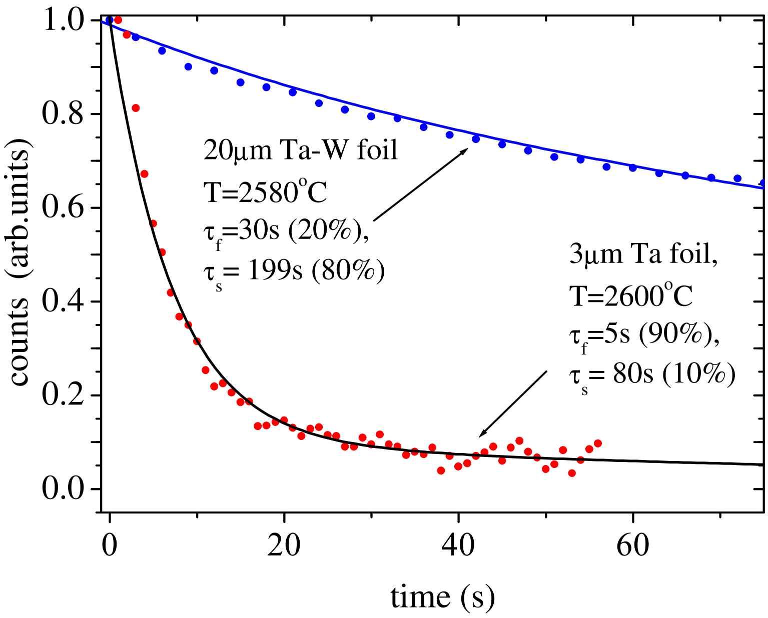


**Fig. 5.** $^{6}Li$ release curves obtained from 3 and 20 $\mu$m foils

In Table 2 Li isotope yields from 20 $\mu$m and 3 $\mu$m thick foils as a target material are presented.

*Table 2*

Yields of lithium isotopes from different target materials

| Isotope | Half-life, Ms | Ta-W foils 20 $\mu$m (5 g/cm$^2$) | Ta foils 3 $\mu$m (1.5 g/cm$^2$) |
|---|---|---|---|
| $^8$Li | 840 | $6\times10^6$ s$^{-1}$ | $1.1\times10^7$ s$^{-1}$ |
| $^9$Li | 179 | $3\times10^5$ s$^{-1}$ | $9\times10^5$ s$^{-1}$ |
| $^{11}$Li | 8.3 | $5\times10^2$ s$^{-1}$ | |

Hence, diffusion can be considered as the main process responsible for release of alkali isotopes from high temperature targets. Thus the diffusion half-time $\tau_{diff}$ extracted from the fit (see Fig. 4) can be taken as a characteristic of the lithium release from the target.

Analysis of the fitted release curve on the Fig. 4 gives the relative amounts $R$ of $^6$Li, escaping from the target with different delay times (Table 3). If the escape process of a nuclide produced in the target is considered to be a diffusion one, the radioactive atom loss coefficient, or probability of escape of radioisotope before decaying is given by M.Fujioka and Y.Arai (Nucl. Instr. Meth. **186**, 409 (1981)):

$$K = \frac{1}{\pi} \cdot \sqrt{\frac{T_{1/2}}{\tau_{diff}}} \tanh\left( \pi \cdot \sqrt{\frac{\tau_{diff}}{T_{1/2}}} \right),$$

where $T_{1/2}$ – half-life of diffusing nuclide and $\tau_{diff}$ – diffusion half-time. Then production efficiency for Li isotopes, corrected on delay, is $\varepsilon = K\times R$. Values of these efficiencies are presented in Table 3.

*Table 3*

Relative amounts of $^6$Li and production efficiencies for radioactive Li isotopes, escaping from the target with different delay times

| Release component $\tau_i$, s | Relative amount $R$ of $^6$Li, % | $\varepsilon$ of $^8$Li, % | $\varepsilon$ of $^9$Li, % | $\varepsilon$ of $^{11}$Li, % |
|---|---|---|---|---|
| 0.071 | 0.03 | $2.0\times10^{-2}$ | $1.4\times10^{-2}$ | $3.3\times10^{-3}$ |
| 14 | 2.73 | $2.1\times10^{-1}$ | $1.1\times10^{-1}$ | $2.2\times10^{-2}$ |
| 120 | 97.24 | 2.0 | 1.2 | $2.5\times10^{-1}$ |

It's clear that we should take into account in our experiment mainly the longest delay time when consider the Li release time influence on the yield of $^8$Li, $^9$Li and even $^{11}$Li.

The component with the shorter delay time would give a noticeable contribution to the yield of produced isotope only when relative amount $R$ of this component is comparable with the amount of nuclides which are released with the longer delay times.

### 2.3. Yields and release of neutron deficient rare earth isotopes

For these tests a high temperature target of a special construction was used, in which the target and ionizer were combined in the same volume. The tantalum foil thickness was 30 $\mu$m. The target mass was 1.5 g/cm$^2$. The yields obtained at the target temperature 2500°C are presented in the second column of Table 4. In the third column of Table 4 the yields of some rare earth nuclides are presented which were obtained from Ta/W sandwich target with the foil thickness 20 $\mu$m at the same temperature. The target mass was 20 g/cm$^2$.

*Table 4*

Yields of rare earth isotopes from different target mass

| Isotope | Yield, $s^{-1}$ target mass 1.5 g/cm$^2$ proton beam intensity 0.1 $\mu$A | Yield, $s^{-1}$ target mass 20 g/cm$^2$ proton beam intensity 0.1 $\mu$A |
|---|---|---|
| $^{156}$Yb | $3.6\times10^4$ | |
| $^{155}$Yb | $1.8\times10^2$ | $6\times10^3$ |
| $^{153}$Yb | $1.0\times10^2$ | |
| $^{158}$Lu | $1.1\times10^5$ | |
| $^{157}$Lu | $5.6\times10^4$ | |
| $^{153}$Yb | $5\times10^2$ | |
| $^{154}$Tm | $2.7\times10^3$ | $4.3\times10^4$ |
| $^{153}$Er | | $3\times10^5$ |
| $^{151}$Dy | | $1.8\times10^6$ |
| $^{151}$Ho | $1.7\times10^6$ | |
| $^{144}$Eu | $>10^6$ | |

The ratio of the yields of $^{155}$Yb and $^{154}$Tm measured from both targets show that the target mass increase gives a proportional rise (within the yield measurement errors) of the yield of short lived rare earth nuclides. In Fig. 6 the delay curve of $^{155}$Yb measured at a temperature 2700°C is shown.

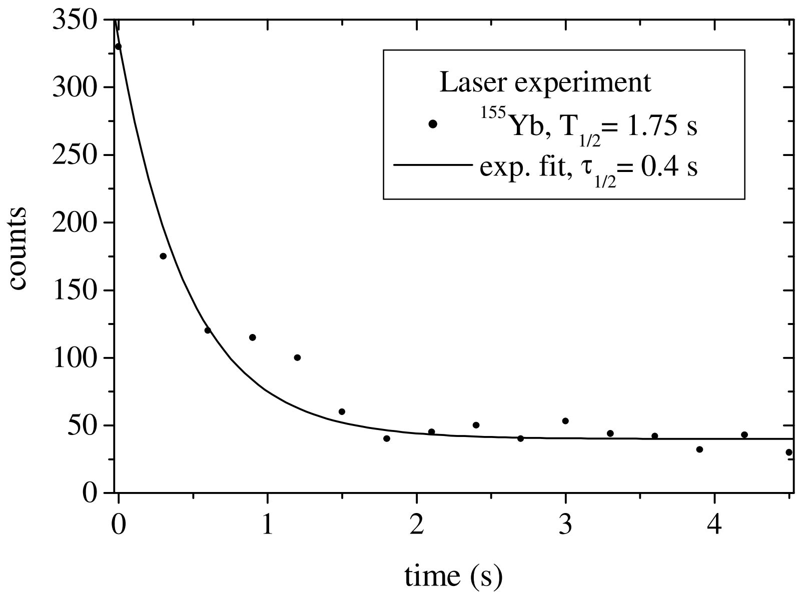


**Fig. 6.** $^{155}$Yb release curve obtained at a temperature 2700°C from 20 $\mu$m foils

### 2.4. On-line tests of a high temperature refractory metal carbide targets. Yields and release of some alkali isotopes

For these tests special high temperature targets have been constructed, which allowed to maintain a metal carbide powder as a target material ($TaC_2$ and $NbC_2$) at a temperature up to 3080°C.

In Fig. 7 the construction of a high temperature metal carbide target is shown in which a low density powder and a high density blocks of a target materials have been used.

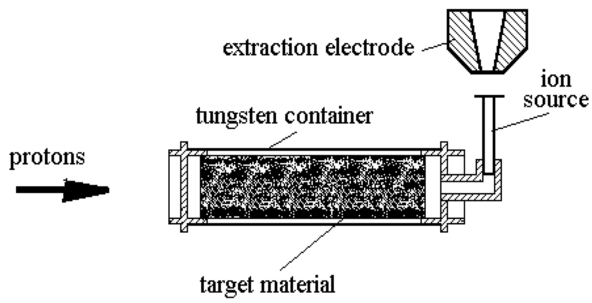


**Fig. 7.** Conceptual scheme of a high temperature metal carbide target unit

The main problem, when that kind of target material is used for a long period (70–100 hours) during on-line run at a temperature of 2300–2500°C, was the carbonization of the target container and its destruction during the experiment. The final construction in which the target material packed into a graphite container which completely isolated from a hot tungsten container allowed to carry out on-line runs of 100 hours duration at a temperature of 2300–2500°C. In Table 5 the yields of Rb and Cs isotopes produced in a high density (11 g/cm$^3$) $UC_x$ target are presented.

***Table 5***

Yields of Rb and Cs isotopes from a high density $UC_x$ target

| Isotope | Half-life | $UC_x$ target 31g/cm$^2$, 0.1 $\mu$A |
|---|---|---|
| $^{143}$Cs | 1.8 s | $1.5\times10^7$ s$^{-1}$ |
| $^{144}$Cs | 1 s | $9.6\times10^6$ s$^{-1}$ |
| $^{145}$Cs | 0.6 s | $4.2\times10^6$ s$^{-1}$ |
| $^{146}$Cs | 0.3 s | $2.4\times10^6$ s$^{-1}$ |
| $^{147}$Cs | 0.2 s | $5.4\times10^5$ s$^{-1}$ |
| $^{148}$Cs | 158 ms | $2\times10^5$ s$^{-1}$ |
| $^{149}$Cs$^*$ | 112 ms | $4.8\times10^4$ s$^{-1}$ |
| $^{150}$Cs$^*$ | 82 ms | $1.2\times10^4$ s$^{-1}$ |
| $^{151}$Cs$^*$ | | $9\times10^3$ s$^{-1}$ |
| $^{95}$Rb | 377 | $6\times10^6$ s$^{-1}$ |
| $^{96}$Rb | 199 | $6\times10^6$ s$^{-1}$ |
| $^{97}$Rb | 170 | $2.4\times10^6$ s$^{-1}$ |
| $^{98}$Rb | 114 | $1.6\times10^6$ s$^{-1}$ |
| $^{99}$Rb | 50.3 | $3.2\times10^5$ s$^{-1}$ |
| $^{100}$Rb | 51 | $9\times10^4$ s$^{-1}$ |
| $^{101}$Rb | 32 | $1.2\times10^4$ s$^{-1}$ |
| $^{102}$Rb | 37 | |

- The yields are given as preliminary ones.

In Fig. 8 the delay curve of $^{80}Rb$ from a niobium carbide target is presented.

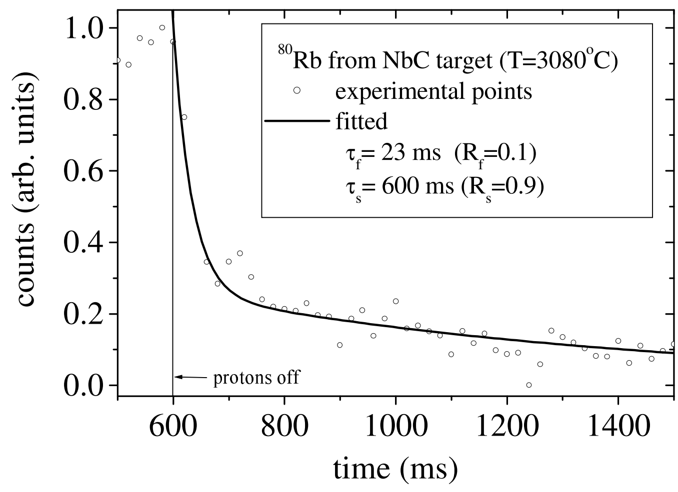


**Fig. 8.** $^{80}Rb$ release curve obtained at a temperature 3080°C $NbC_x$ target

In Figs. 9, 10 the release curves of radiogenic $^{7}Li$ escaping from $TaC_x$ and $NbC_x$ targets are presented. The delay time for Rb isotopes measured from $NbC_x$ powder target is the shortest one of the measured so far. That kind of target can be the most effective tool for production of short lived neutron deficient isotopes of Rb. Refractory metal carbide targets have shown a very high stability when being maintained at a high temperature and can be the fastest and most efficient target for short lived neutron deficient isotope production.

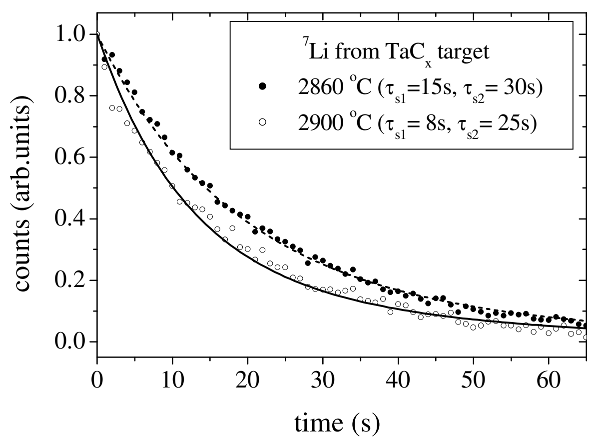


**Fig. 9.** Release of $^{7}Li$ from a high temperature $TaC_x$ target

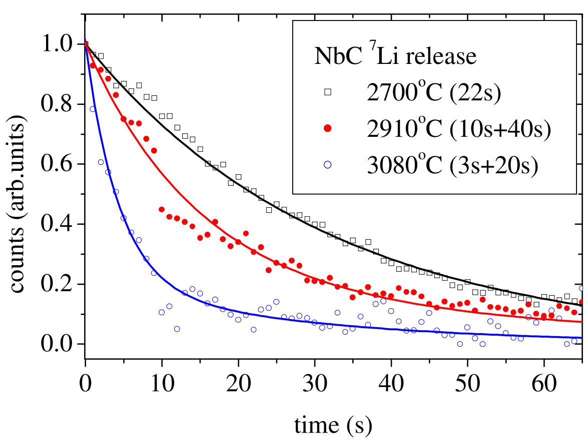


**Fig. 10.** $^{7}Li$ release curves from a high temperature $NbC_x$ target

## 2.5. The use of a neutron generator effect for two step neutron rich isotope production

The effect of a neutron generator, when the proton beam is directed to the tantalum block, placed close by the $UC_x$ target, was used for production of neutron rich Rb and Cs isotopes in two-step reaction.

For on-line tests two kinds of targets of different density ($UC_x$ powder 3.1 g/cm$^3$ and $UC_x$ blocks 11 g/cm$^3$) placed into a tungsten container heated by the ohmic heating up to the temperature of 2500°C have been used [6].

In Fig. 11 the schematic view of the target area with a tantalum block placed close to the target for the secondary neutron flux generation is shown. In the same experiment the proton beam was directed to the $UC_x$ powder target (direct production by protons), or to the tantalum block (indirect production by neutrons).

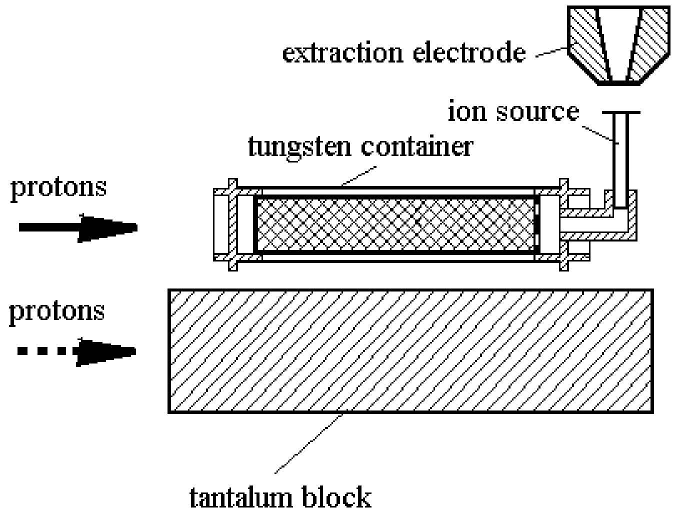


**Fig. 11.** Schematic view of the target area with a tantalum block placed close to the target

In Fig. 12 Cs and Rb isotope yield ratios when the proton beam irradiated the tantalum block or $UC_x$ powder target are presented.

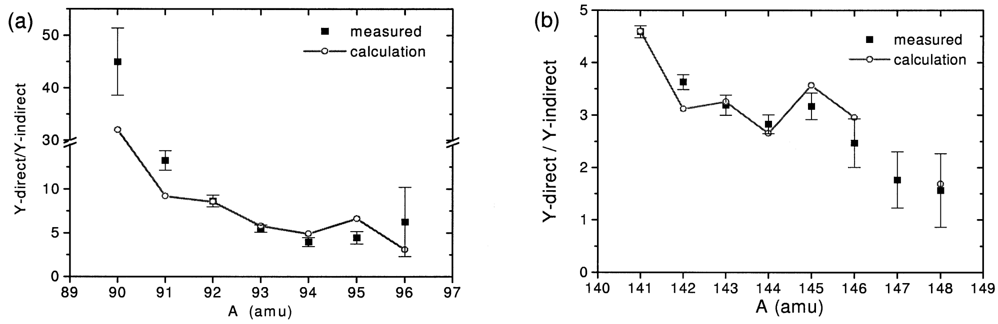


**Fig. 12.** Plots of Rb (a) and Cs (b) isotope yield ratios in direct and indirect production scheme. Calculation are performed by J.Nolen, I.Gomes and M.Portillo (Sci. Instr. Rev., to be published)

The same effect of the influence of secondary neutron production inside the high density target on the yield of neutron deficient Cs isotopes is shown in Fig. 13.

The yields of neutron rich Cs isotopes far from stability from a high density $UC_x$ target rise about five times as compared to the yields from a powder $UC_x$ target of a low density.

The experiments with the use of two step reaction when neutron rich isotopes in $UC_x$ target are produced by secondary neutrons have shown a very good perspective for rise of the production yields of all produced neutron rich nuclides.

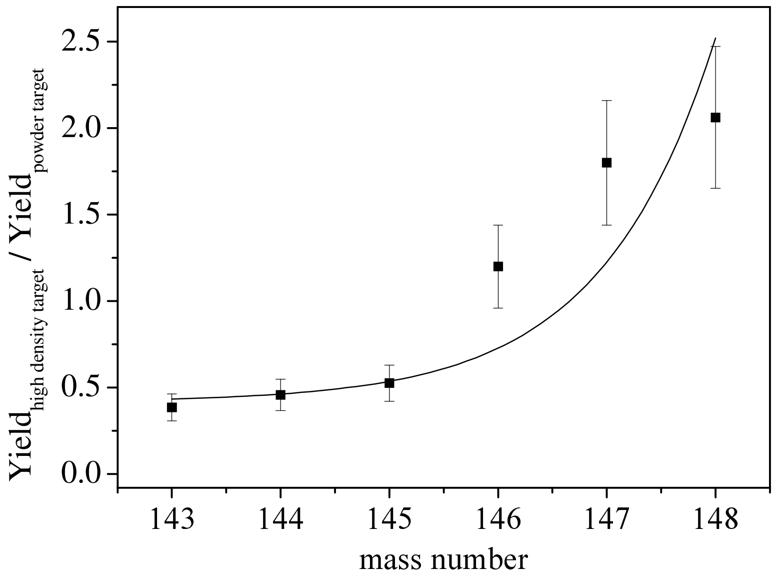


**Fig. 13.** Plot of the yield ratios for Cs isotopes

## 3. Development of the laser and high temperature electron bombardment ion sources

### 3.1. High selective laser ion source development

As it has been shown by the experiments with a laser ion source, it is a very good instrument not only for selection of isobars produced, but also for the laser spectroscopic investigations. The main problem that seriously limits the laser ion source application for that purpose is a drastic decrease of its selectivity, when it works at a high temperature (>1800°C), or is coupled with a high temperature target due to a high thermoion current from the target volume and laser ion source cavity. At IRIS facility a series of off-line and on-line tests have been carried out that ensured the high temperature target – laser ion source assembly selectivity rise of about two orders of magnitude. The new developed methods made it possible to carry out spectroscopic measurements of neutron deficient Yb and Tm isotopes and can be used for selective production of many other nuclides.

### 3.2. Off-line and on-line tests of the high temperature target – laser ion source unit

In Fig. 14 a conceptual scheme of a high temperature target – laser ion source assembly is presented. The working target temperature for rare earth isotope production was 2500–2800°C. The laser ion source tube has a length of about 50–60 mm and usually maintains at a temperature 1800–2000°C. In Fig. 15 a tungsten laser ion source selectivity temperature dependence is shown. The selectivity values of laser ion source tubes made of Nb and TaC are presented as well at a temperature 1900°C.

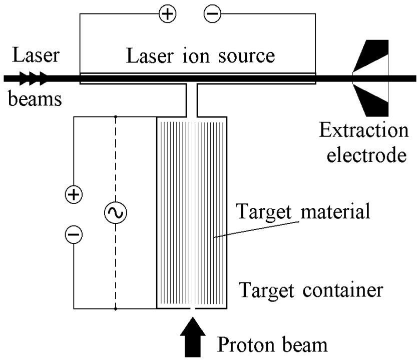


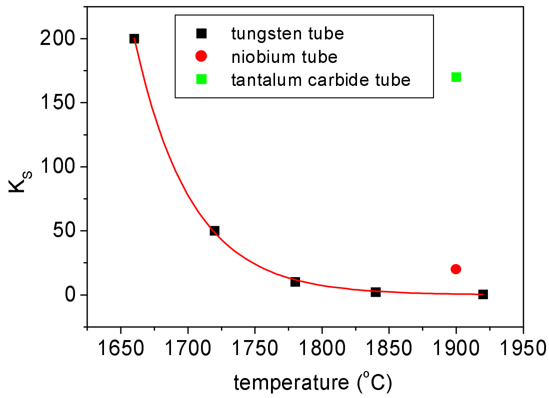


**Fig. 14.** Scheme of a high temperature target – laser ion source assembly

**Fig. 15.** Laser ion source selectivity temperature dependence

When the laser ion source is coupled with a high temperature target, the selectivity of such a system can be represented by the following way [7]:

$$S = K_B \cdot \frac{I_L}{I_T} = K_B \cdot K_S ,$$

where $K_B$ – ratio of the period of laser pulses to the duration of ion bunches produced by the laser light and extracted from the ion source. $I_L$ – the current of the investigated isotope ions produced by the laser ionization (selective signal). $I_T$ – is the current of the same isotope and its isobar thermoions produced by the surface ionization inside the volume of the laser ion source and in the target volume (nonselective signal).

Off-line tests have shown that during a long heating process (of about 15 hours) the carbonization of the inner surface of the laser ion source capillary heated inside a graphite tube takes place that gives a considerable decrease of its workfunction and increase of selectivity. By this method the laser ion source selectivity can be risen by a factor of 50. In Fig. 16 the $K_S$ value dependence on the heating time of a thin tantalum capillary placed into graphite tube is presented.

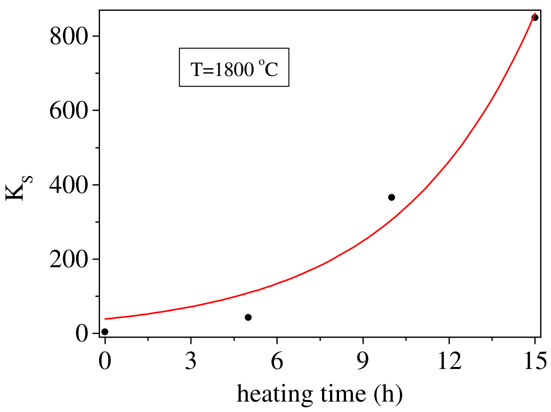


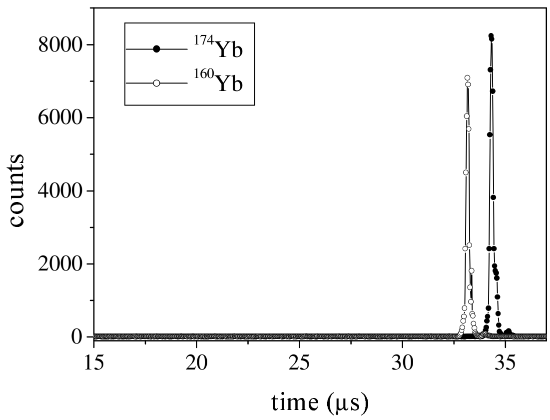


**Fig. 16.** $K_S$ value dependence on the heating time

**Fig. 17.** Bunches of stable $^{174}$Yb and radioactive $^{160}$Yb isotopes

For the purpose of selectivity rise the inner surface of a high temperature target should be carbonized as well, or a thermoion background suppression method [7] should be applied. Another very efficient way of the selectivity increase is the use of the time structure of the ion beam produced by the laser light pulses. As it was shown by the latest experiments at IRIS, the $K_B$ value can reach 100. In Fig. 17 the bunches of stable $^{174}$Yb and radioactive $^{160}$Yb isotopes produced in a tungsten laser ion source 1.5 mm in diameter are shown.

The HTR target – laser ion source unit selectivity was risen by a factor of 20 by applying the thermal ion closing potential [7]. In off-line tests the selectivity of laser ion source made of thin tantalum foil rises of about 50 times due to the carbonization of the laser ion source inner surface. As it was shown by off-line and on-line tests, the use of the time structure of the beam of laser ionized atoms can ensure the value of selectivity increase by a factor of 100.

### 3.3. High temperature electron bombardment ion source for ionization of isotopes of all elements of the Periodical Table

First on-line tests of a high temperature electron bombardment ion source (HTEBIS), coupled with $UC_x$ powder and $UC_x$ block targets have been carried out. A number of isotopes: $^{58\text{-}60}$Mn, $^{113\text{-}119}$Ag, $^{119,121}$Cd, $^{119\text{-}125}$In, $^{127\text{-}132}$Sn, $^{192,196}$Tl, $^{196\text{-}199}$Pb, $^{196}$Bi, $^{197\text{-}200}$Po and $^{201,203}$At were produced making use of a high temperature electron bombardment ion source (see Fig. 18).

The ionization efficiency obtained making use of HTBIS in off-line and on-line tests is 0.5–2% without an axial magnet field applying. Off-line experiment with axial magnet field of 200 Gauss use for the electron rotation gives the efficiency value rise of about one order of magnitude. As the working temperature of that kind of ion source is very high (up to 2500–2800°C), it can be used for ionization of practically all elements of the periodical table. In Fig. 19 the influence of secondary neutron generation effect on the yield of neutron rich In isotopes from $UC_x$ high density target coupled with HTEBIS is shown. One can see from Fig. 19 that the yield ratios for In isotope yields produced in $UC_x$ high density target to the yields from $UC_x$ powder target are rising about five times when going to the neutron rich side from stability line. It shows that the secondary neutron generation effect ensures the rise of not only neutron rich Rb and Cs isotopes but very likely is valid for all neutron rich isotopes produced in $UC_x$ targets.

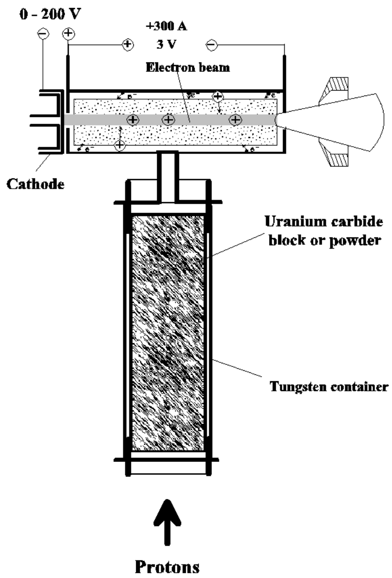


**Fig. 18.** $UC_X$ target coupled with the high temperature electron bombardment ion source

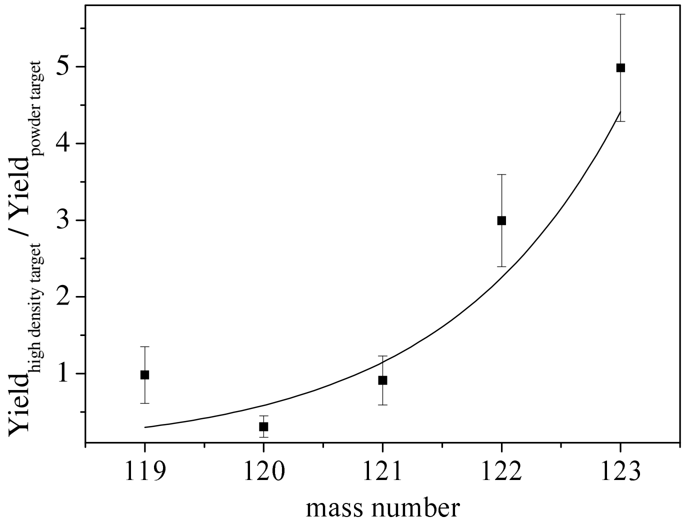


**Fig. 19.** The yield ratios for In isotope yields produced in $UC_x$ high density target to the yields from $UC_x$ powder target

## 4. Conclusion

The escape process of Li from high temperature refractory target at a temperature higher 2400°C is mainly a diffusion one.

The yields of alkali isotopes from a high temperature refractory target can be risen by the target temperature increase, the target material surface carbonization (protection against sticking) and by the use of thinner foils.

The use of a neutron generation effect ensures a considerable production gain of neutron rich isotopes from uranium carbide targets.

High density uranium carbide target seems to be a very effective tool for production of a large set of nuclides both from neutron rich and neutron deficient side of nuclide chart.

Due to a neutron generation effect inside the high density $UC_x$ target volume that type of target can be more effective than $UC_x$ powder target in production of neutron rich isotopes far from stability.

The use of a High Temperature Electron Bombardment Ion Source (HTEBIS) has appeared to be rather promising for production of a large number of nuclides with different physical and chemical properties.

The high temperature target-laser ion source unit selectivity was risen by a factor of 20 by applying the thermal ion closing potential.

In off-line tests the selectivity of laser ion source made of thin tantalum foil rises of about 50 times due to the carbonization of the laser ion source inner surface.

As it was shown by off-line and on-line tests, the use of the time structure of the beam of laser ionized atoms can ensure the value of selectivity increase by a factor of 100.

Full list of participants:
V.N.Panteleev, A.E.Barzakh, Yu.S. Blinnikov, D.V.Fedorov, T.T. Fedorov, V.S. Ivanov, G.G.Lemeshko, F.V.Moroz, S.Yu.Orlov, A.G.Polyakov, M.D.Seliverstov, Yu.M.Volkov.

## Acknowledgements

We would like to thank D.M.Seliverstov for encouragement and support to our work.

## References

[1] G.D.Alkhazov, E.Ye.Berlovich, and V.N.Panteleev, Nucl. Inst. Meth. **A 280**, 141 (1989).
[2] G.D.Alkhazov *et.al.,* Nucl. Inst. Meth. **A306**, 500 (1991).
[3] G.D.Alkhazov *et.al*., Nucl. Inst. Meth. B69, 517 (1992).
[4] V.N.Panteleev *et.al.,* Preprint PNPI-2306, Gatchina, 1999, 17 p.
[5] A.E.Barzakh *et.al*., Phys. Rev. **C61**, 034304 (2000).
[6] V.N.Panteleev *et.al*., in *Proc. Int. Conf. on Exotic Nuclei and Atomic Masses (ENAM 2001),Hameenlinna, Finland, 2−7 July 2001.*
[7] V.N.Panteleev *et. al*., Hyper. Int. **127**, 421 (2000).